APPLICATION OF MESH SHEET ENERGY DIRECTORS TO ULTRASONIC WELDING AND SINGLE LAP JOINT STRENGTH OF CF/PPS COMPOSITES

Shin-ichi Takeda[1], Jonathon D. Tanks[2], Sunao Sugimoto[1] and Yutaka Iwahori[1]

[1]Advanced Composite and Structures Unit, Aeronautical Technology Directorate, Japan Aerospace Exploration Agency, 6-13-1 Osawa, Mitaka-shi, Tokyo 181-0015, Japan
Email: takeda.shinichi@jaxa.jp, sugimoto.sunao@jaxa.jp, iwahori.yutaka@jaxa.jp,
Web Page: http://www.aero.jaxa.jp/eng/research/basic/structure-composite/
[2]Department of Chemical Science and Engineering, Tokyo Institute of Technology, 2-12-1 Ookayama, Meguro-ku, Tokyo 152-8552, Japan
Email: tanks.j.aa@m.titech.ac.jp, Web Page: http://www.chemeng.titech.ac.jp/~tklab/index-e.html

Keywords: CFRTP, Ultrasonic welding, Single-lap joints

Abstract
Ultrasonic welding technology for thermoplastics has developed quickly in recent years. For aircraft structural applications, this joining technique shows promise over standard epoxy adhesives, resistance welding, or mechanical fastening in terms of scalability and efficiency. However, identification of optimal ultrasonic welding parameters remains a difficult task. Energy directors with either flat or custom-made geometries have been the focus of much recent research, but a clear winner has not yet emerged. In this study, single-lap joints (SLJ) of unidirectional CF/PPS laminates were manufactured by ultrasonic welding, using commercially available PPS mesh inserts as energy directors. The shear strength was evaluated, and the failure surfaces were examined to understand the relationship between welding parameters and resultant strength. Results indicate that coarser mesh size, along with longer welding times, tend to result in higher SLJ shear strength.

1. Introduction

Non-mechanical fastening techniques for joining carbon fiber reinforced thermoplastic (CFRTP) composites in aircraft structures are of interest for the sake of weight-saving and manufacturing flexibility. Adhesive bonding is most commonly used, typically epoxy-based, and various surface treatment methods have been studied [1]. However, an alternative to adhesives for the case of CFRTP is welding. The main categories include induction welding, resistance welding, and ultrasonic welding [2]. Ultrasonic welding in particular shows promise for industrial application due to speed and low energy consumption [3]. Some studies show average SLJ shear strengths between 30-35 MPa, depending on the adherend composite type and the thermoplastic used in the joint [2-5]. A thermoplastic material is inserted between the adherend plates in order to improve the efficiency of melting and produce a stronger bond is called an energy director (ED) [4-5]. Numerous configurations have been tested for EDs, including flat vs. sharp, single vs. multiple; however, while the flat EDs tend to be easy to install during welding, the more complex geometries can be time-consuming or costly to fabricate. In this study, a commercially available PPS mesh was used as the ED material, varying the mesh size in order to assess its potential for improving ultrasonically welded CFRTP joints. The woven pattern of the mesh provides concentrated contact points for directing the welding energy. No special equipment or ED installation time is required for this simple method.

2. Preparation of CF/PPS single-lap joint specimens

Single-lap joint (SLJ) specimens were prepared from unidirectional CF/PPS laminates using the ultrasonic welder (ΣG2210SS/DΣP80SS, SEIDENSHA ELECTRONICS CO., LTD.). The CFRTP was manufactured by vacuum hot press using the UD prepregs (Cetex TC1100, Koninklijke Ten Cate B.V.). The stacking sequence was $[0]_{10}$ and the resulting plates with thickness of roughly 1.6 mm were cut to sizes of 30 × 100 mm. Rather than use custom-made energy directors, commercially-available PPS mesh of different fineness was used as insert materials shown in Figure 1; the details of mesh geometry are shown in Table 1. One series also includes a double layer of the #100 mesh.

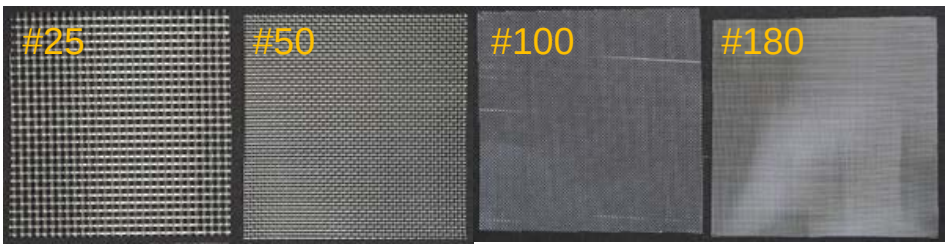

Figure 1. Appearances of PPS mesh sheets.

Table 1. Details of PPS mesh inserts used as energy directors.

Mesh size (Wire/inch)	Wire diameter (μm)	Aperture (μm)	Sheet thickness (μm)
25	280	723	510
50	150	358	280
100	55	200	100
180	34	100	68

To explore the effect of mechanical surface treatment (i.e., non-chemical treatment), each specimen series was duplicated with the welding surfaces of the CFRTP having been sanded with #240-grit SiC paper. The details for all welding parameters are listed in Table 2. The specimen labeling system is as follows: [Mesh size]-[surface treatment]-[welding time]. Surface treatment is indicated by "N" (no treatment) or "S" (sanding surface treatment). Replicate specimens of each series are labeled by an additional digit of 1 through 5.

Table 2. Test matrix of welded specimens (pressure = 1.1 MPa; holding time = 5 sec).

Welding time (sec)	Surface treatment	Mesh sheets					
		N/A	#25	#50	#100	#100 ×2	#180
1	N/A	5			5		5
	#240 sanding	5			5		5
2	N/A			5	5	5	
	#240 sanding			5	5	5	
3	N/A		5				
	#240 sanding		5				

Several specimens with welding times of 2-3 sec showed excessive melting of the PPS matrix in the CFRTP plate, causing the carbon fibers to spread outward on the side edges, as shown in Figure 2. The outer surfaces (i.e., opposite the inner surfaces of the joint) showed no such deformation. Of these specimens, the observed tendency was for finer mesh (e.g., #100) to undergo higher degree of melting and deformation, as compared with coarser mesh (e.g., #25). This is because of the energy required to melt a larger quantity of PPS mesh resin, which diverts the energy from melting the CFRTP matrix. Welded assemblies had a width of 30 mm, in order to cut away the deformed edges and produce uniform SLJ test coupons with width of 25 mm. The lap lengths were between 11-13 mm, which was considerably variable.

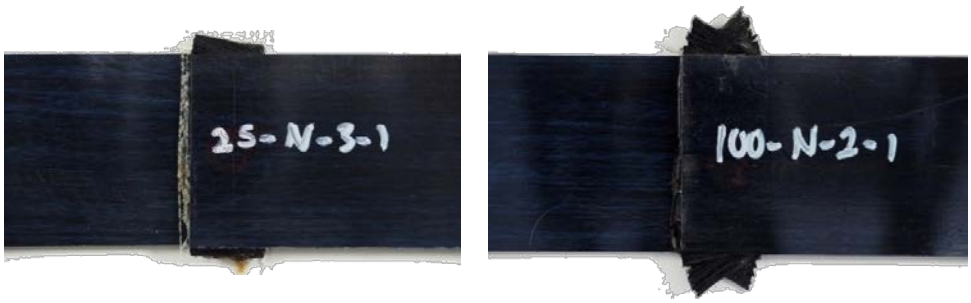

Figure 2. Examples of plate deformation due to excessive melting during welding.

3. Evaluation of Lap Shear Strength

All specimens were prepared and testing in an identical manner. Using a servohydraulic universal test machine (max. capacity = 100 kN), SLJ tests were performed according to ASTM D3165. A clip-on type extensometer (gauge length = 25 mm) was used to measure shear displacement between the two plates. Several trial specimens were tested in order to confirm there was no slippage of the grips or other errors.

The summary of single lap joint shear strengths for each welding condition is shown in Figure 3. The “apparent” and “true” shear strengths were calculated from the experimental force data using either the nominal welded area or the true (measured) welded area, respectively. This allows the effects of different manufacturing parameters to be more consistently compared by controlling for welded area.

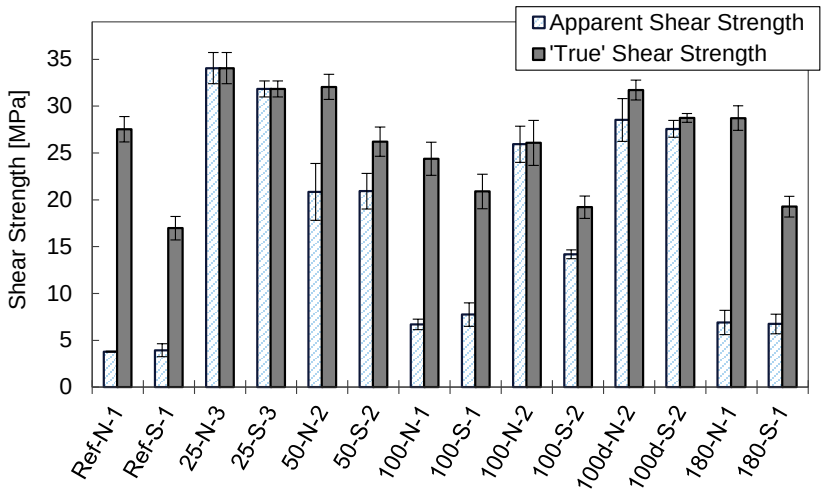

Figure 3. Summary of shear strengths for nominal (‘apparent’) and measured (‘true’) welded areas.

From this graph, two main observations were made. First, the most obvious indicator of higher shear strength is the amount of PPS resin available during welding; i.e., mesh sizes #25, #50, and doubled #100 show the highest shear strengths. For the two conditions with smaller amounts of PPS resin, #180 and single #100, the trend is reversed so that #180 mesh shows higher strength. Based on the results shown in Section 4, this is likely because cohesive failure is dominant for #180, while #100 shows mostly cohesive failure with some scattered adhesive failure. Second, the effect of surface treatment by sanding (#240-grit SiC sandpaper) is negative, resulting in lower shear strength than the no-treatment condition for all mesh types. This is due to the removed resin layer in the treated specimens, so that less PPS resin is available for the welding process.

4. Evaluation of Welded Surfaces

Photographs of representative failure surfaces for non-treated specimens are shown in Figure 4, with the exception of 50-S-2, in order to show the difference between treated and non-treated surfaces. Three types of failure surfaces can be seen, namely: (1) unmelted PPS mesh (no contribution to SLJ shear strength), (2) adhesive failure, where a relatively thick resin layer separates from the adherend primarily by Mode II failure, and (3) cohesive failure, where the fully bonded surfaces exhibit failure through the thickness of the thin resin layer. Unfortunately, the selected welding time for reference specimens (1 sec) was too short to join the plates, leaving very small welded regions around the outer edges of the lap area. Clearly, the deformation of the plates caused by excessive melting (shown in Figure 3) is no indication of the actual welded area, since the center of the joint may still have unmelted PPS mesh and thus contribute no strength to the assembly.

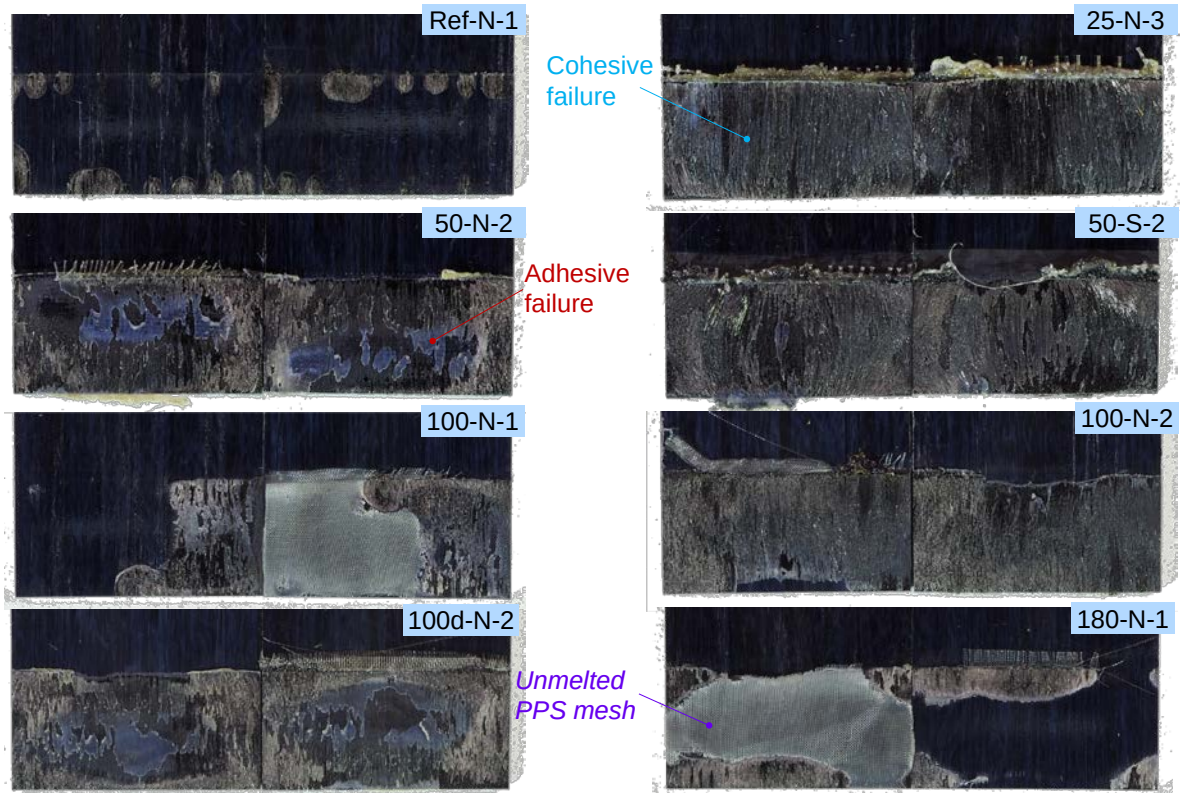

Figure 4. Failure surfaces of SLJ test specimens.

Although comparisons between different mesh sizes and welding times can be difficult due to little overlap in the selected parameters, one clear observation concerning the progression of PPS melting during welding is illustrated in Figure 5. Here, the short welding times (corresponding to fine mesh) result in only partial melting of the PPS mesh, starting at the outer edges and moving inward. Moderate welding times seem to melt the PPS mesh enough that the entire joint is covered, but the centermost region remains as a relatively thick resin layer that is adhered to the CFRTP plates. Finally, for the longest welding time (corresponding to coarse mesh), the PPS mesh is completely melted and blended with the PPS matrix of the CFRTP plate, such that the carbon fibers of both plates nearly entangle as one solid plate. Thus, the failure mode tends to follow this progression, so that the cohesive failure zone steadily spreads from the outward edges toward the center as the welding time increases.

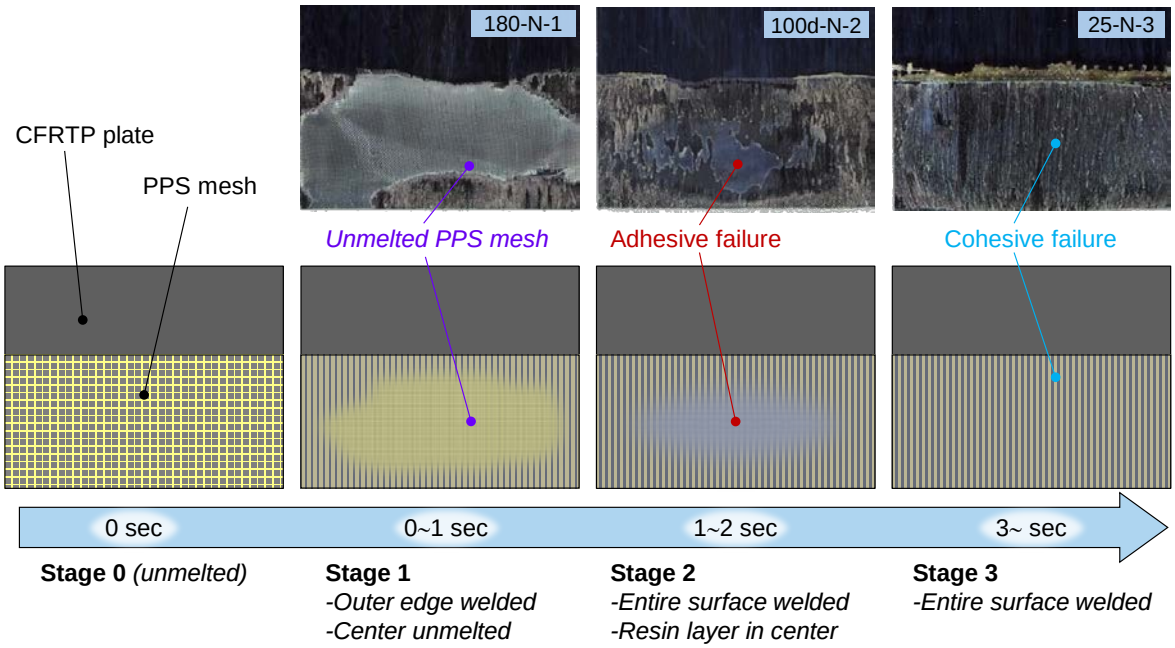

Figure 5. Progression of PPS melting during ultrasonic welding and associated failure modes.

The ultrasonic power as recorded by the welding machine is shown in Figure 6 by representative samples. Typically, the power increases as frictional and vibrational energy is dissipated and temperature inside the joint region increases, until the PPS resin softens sufficiently that viscoelastic energy dissipation initiates and starts melting the resin, which starts approximately at the peak power. The time required to reach this peak varies for each mesh type and surface treatment; i.e., the total (cumulative) energy required is dependent on (1) the amount of PPS resin available for melting, (2) the energy directing efficiency, and (3) the surface condition of the CFRTP plate. For example, consider the specimens 100-N-2 and 100d-N-2. The energy directing behavior should be roughly the same since the mesh is the same, but the mass quantity of PPS resin is double for 100d-N-2. Thus, more time is required to reach the peak power for 100d-N-2 (~1.6 sec) compared to 100-N-2 (~1.2 sec). For the finer meshes, peak power is not reached, and thus the unmelted regions shown in Figure 4 can be understood. However, given that the specimens with more coarse mesh (#25, #50, #100d) exhibit a lower peak power than the finer mesh series (single #100, #180), it seems that the coarser mesh sizes exhibit better energy directing performance. This is indicated by the smaller slopes of the pre-peak portion of the power-time curves, where the trend for smaller slope is given by #25 < #50 < #100d. The noticeable effect of sanding surface treatment is a reduction in the peak power for the joints with fine mesh. This may be due to more uneven contact between the fine mesh and the rough surface of

the CFRTP plate, which allows for more efficient energy directing. However, the effect is negligible for coarser mesh sizes.

The normalized welded area—measured by image analysis of all failure surfaces—and the adjusted SLJ shear strength are plotted against the total welding energy (i.e., integral of power curves in Figure 6) in Figure 7. Generally, the welded area increases as the energy increases, until a fully welded joint is achieved above some required energy which depends on the mesh size. This holds true for both non-treated and treated surfaces. However, although the SLJ shear strength also follows a linear trend with welding energy, the specimens with sanded surface treatment exhibit lower strength regardless of welded area. This use of normalized area and corrected strength allow the inherent strength of each welding condition to be compared, rather than including the effect of welding efficiency. Note the relatively low strength of 100-N-2, despite over 98% welded area. A single layer of #100 mesh results in an inherently weaker joint, while double layer #100 gives over 20% higher strength for the same welding time. Furthermore, recalling Figure 4, despite 100-N-2 having larger cohesive failure zones than 100d-N-2, the strength is lower. Considering also the high strength of 25-N-3 and its primarily cohesive failure behavior, as well as the consistently lower strength resulting from sanding surface treatment, and it is reasonable to conclude that the shear strength of ultrasonically welded joints is predominantly influenced by the mass quantity of PPS resin available for melting during the welding process. All other factors held constant, this appears the most important.

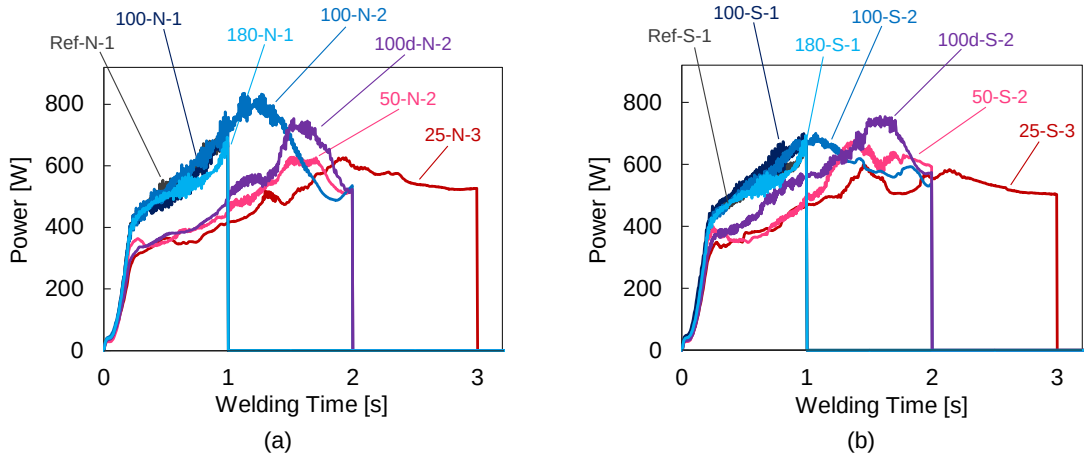

Figure 6. Ultrasonic power evolution during welding for (a) no treatment, and (b) sanded treatment.

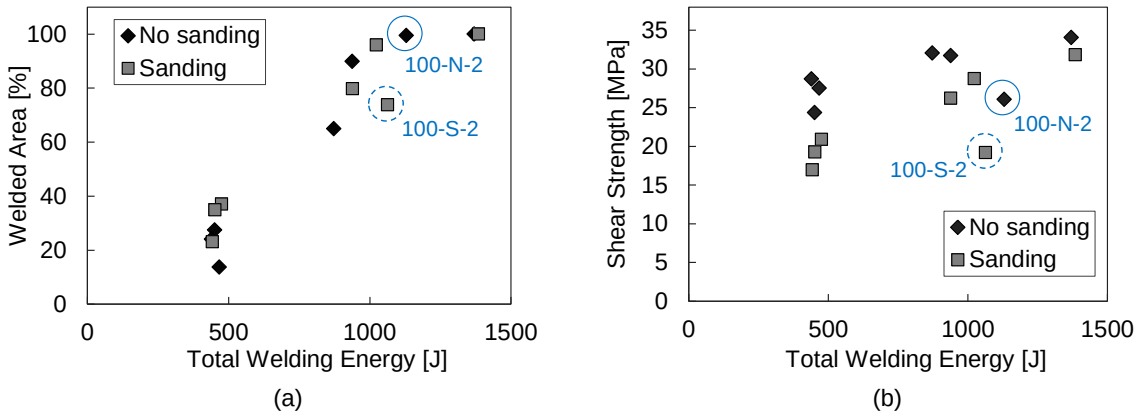

Figure 7. Dependence of (a) welded area, and (b) SLJ shear strength, on the total welding energy (calculated by integration of the power-time curves in Fig 6).

5. Conclusions

In this study, single-lap joints (SLJ) of unidirectional CF/PPS laminates were manufactured by ultrasonic welding, using commercially available PPS mesh inserts as energy directors. The shear strength was evaluated, and the failure surfaces were examined to understand the relationship between welding parameters and resultant strength. Several observations were made from these results.

Firstly, sanding surface treatment of the CFRTP plates has a negative effect on shear strength. This is believed to be caused by the removal of the resin-rich layer and thus there is less PPS available for melting during welding. It is not recommended for future study as an experimental parameter.

Secondly, it is impossible to judge the condition of the welded region based on visual observation of the coupon after welding. Deformation of the carbon fibers at the edges of the CFRTP plates—due to excessive melting of the PPS matrix—was observed for many specimens, yet internally the welded area was much smaller than the nominal area. Non-destructive evaluation (NDE) techniques should be considered for inspecting ultrasonic welds in future scaled-up operations.

Thirdly, when correcting for partial-welding due to short welding times, coarser PPS mesh size produces higher SLJ shear strength compared to finer mesh. This is most likely due to the difference in the amount of PPS resin available for melting during welding; additionally, coarser mesh shows improved energy directing performance over fine mesh, requiring less power to initiate melting.

Finally, the melting process tends to start at the edges of the joint and move toward the center. Longer welding time is required to fully melt the resin for coarser mesh sizes, but unless the mesh efficiently directs energy to initiate welding at lower power levels, the PPS matrix in CFRTP plate itself begins to melt and results in noticeable deformation. This was observed for the case of fine PPS mesh, where the welding time was short so that welding occurred only at the outer edges while the center remained unmelted, yet the edges of the CFRTP plate showed significant deformation. For this reason also, in addition to the consideration for joint strength, coarser mesh sizes is recommended for future study.

References

[1] Tetsuo Yasuoka , Tomo Takeda, Hikaru Hoshi, Sunao Sugimoto and Yutaka Iwahori. Wettability, surface geometry and adhesively-bonded joint strength of various surface treatments on titanium alloys or CFRP. *JAXA Research and Development Report*, JAXA-RR-16-014, ISSN 1349-1113, 2017 (in Japanese).

[2] O'Shaughnessey, P.G., Dube, M., and Villegas I.F.. Modeling and experimental investigation of induction welding of thermoplastic composites and comparison with other welding processes. *Journal of Composite Materials*, 50:2895–2910, 2016.

[3] Senders, F., van Beurden, M., Palardy, G., and Villegas, I.F.. Zero-flow: A novel approach to continuous ultrasonic welding of CF/PPS thermoplastic composite plates. *Advanced Manufacturing: Polymer & Composites Science*, 2: 83-92, 2016.

[4] Villegas, I.F., and Bersee, E.N.. M Zero-flow: Ultrasonic welding of advanced thermoplastic composites: An investigation on energy-directing surfaces. *Advances in Polymer Technology*, 29: 112-120, 2010.

[5] Palardy, G., and Villegas, I.F.. Ultrasonic welding of thermoplastic composites with flat energy directors: Influence of the thickness of the energy director on the welding process: An investigation on energy-directing surfaces. *Proceedings of the 20th International Conference on Composite Materials (ICCM20)*, Copenhagen, 2015.